Comparison of Mixing Performance of Different Types of Passive Micromixers Using Numerical Analysis

Tanveer Rahman[1a], S M Faisal Ahmmed[1b], Zubairul Alam[1c], Moddassir Khan Nayeem[1*]

[1]Department of Industrial & Production Engineering
Military Institute of Science & Technology, MIST
Dhaka, Bangladesh

mknayeem.ie@gmail.com[*], zubairkareeb6928@gmail.com[c], smfaisal824372@gmail.com[b], tanveerrahman45279@gmail.com[a]

Abstract

Micromixers have a wide range of applications in biotechnological engineering, analytical chemistry, medicine, and high-throughput synthesis. Therefore, the study of the micro-mixing channels and flow structures with different geometric patterns is very important. In this study, the comparison of different micromixers with varying geometric patterns namely, Zigzag, Ohm, Z patterns are investigated to evaluate the mixing performance. In order to conduct the numerical investigation, three-dimensional Navier-Stokes equations are employed in conjunction with a convection-diffusion model, which is developed by the researchers. Two working fluids: water and ethanol are used as working substances in both patterns. The results show that the Z and Ohm shape micromixer yields better mixing performance compared with the Zigzag shape. The pressure drop in the Zigzag shape is consistently lower than the pressure drops in the z shape and Ohm shape, demonstrating that the pressure profile in the zig-zag shape is superior to that of two proposed shapes (Z & Ohm). But, with the increasing reduction in mesh size, until it approaches the optimal mesh size of 0.00006, which is the smallest feasible, the outflow velocity of the Zigzag form decreases significantly when compared to both shapes (Z & Ohm), until it reaches the absolute minimum imaginable value. Comparing the result, it can be concluded that the mixing performance Z shape and Ohm shape outperform the Zigzag shape.

Keywords

Micromixers, Fluent, Microchannels, Reynolds Number, Pressure drop

1. Introduction

Microfluidic devices are used in various applications. They are characterized by low volume consumption, high throughput, and flexible operation. Microscale devices are used for biochemical analysis, screening of cancer, monitoring of molecular changes in the environment, the rapid well-mixed reagents. They are usually composed of various components such as pumps, detectors, and scanners. But, due to the small size of the Reynolds number in microfluidic devices, the flow is laminar; turbulent mixing is not an efficient method because the molecular diffusion dominates the mixing performance (Hossain et al., 2009). The versatility of microfluidic systems has helped to improve the scientific fields of study (Tofteberg et al., 2010). In order to speed up the process, some simple steps can be utilized to enhance the mixing performance by creating different geometry or shape.

Recycle reactors are widely used in the chemical industry to achieve high conversion while also reducing reactor volume. To facilitate mixing, a turbulent flow is usually generated. However, due to the laminar flow inside the reactor, fast mixing is extremely difficult in a micro recycle reactor. As a result, to address the mixing issue, we developed a recycle micromixer that can also function as a micro recycle reactor (Jeon et al., 2005). Electrokinetics is one of the most flexible and versatile microfluidic platforms available, as it allows for microfluidic flow control to be achieved through the use of electric fields. When it comes to laminar fluid flow, the microfluid domain has a high surface-to-volume ratio (Kim et al., 2018). The primary mixing process in lab on a chip is diffusion, which occurs in this micro regime because the Reynolds number is very low in this environment (Viktorov & Nimafar, 2013). Systematic

research on slug length and pressure drop has been conducted on the chemically inert water cyclohexane system (Kashid & Agar, 2007). Mass transfer behavior of Y junction micromixer is determined by slug geometry and circulation patterns affected by the physical properties of liquids and operating parameters such as flow rates, mixing element, geometry, and capillary diameters. At varied flow velocities, the pressure drops through distinct Y-junction mixing elements and along the length of each capillary was observed. The power input was evaluated utilizing pressure losses across the mixing element, and it was discovered that the slug flow capillary microreactor outperforms traditional equipment by delivering greater interfacial area with less power.

There are two categories of micromixers: active and passive. Active micromixers with external energy sources provide adequate mixing quality and a fast-mixing process. However, active micromixers using external energy sources such as ultrasonic vibration (Hossain et al., 2009), electrokinetic (Anwar et al., 2010), and gas pressure driving force consists of many parts, complicating the fabrication process and integrating with other microfluidic systems. Passive micromixers do not use external energy sources; instead, they rely on the physical microchannels for fluid mixing, and they have the advantages of stable operation, easy integration and low-cost manufacturing. Most passive micromixers use a single mixing process such as molecular diffusion or recirculation or vortices, split-recombining or transverse flow (Le The et al., 2015).

At low Reynolds numbers, mixing takes a long time because viscous effects from molecular diffusion dominate the mixing of a passive micromixer. Mixing can be improved by modifying the geometry to increase the mixing interface, inducing chaotic advection by creating vortices and increasing the interfacial area between various fluids. So, in this study a new Z & Ohm shape passive micromixer is designed to compare the mixing performance with an existing model (Zig-zag shape) of passive micromixer with the optimal values such as outlet velocity, pressure drops, Re numbers that increases the mixing efficiency**.**

1.1 Objectives

In this work, we have proposed two novel shapes (Z shape and Ohm shape) that have never been proposed before. Then, we will compare our results for each shape with an existing Zigzag shape micromixer concerning Re number, outlet velocity and pressure drop. According to their mixing performance, we will select the most efficient passive micromixer from among the three different shapes of passive micromixers.

2. Literature Review

Passive T-mixers have better mixing performance at higher flow rates. Taylor dispersion type obstructions have been studied to improve the efficiency of the flow of T micromixer But mixing improvement has been significantly reduced for Re greater than 500 while installing the mechanism of Taylor dispersion obstacles (Manoj Dundi et al., 2020). The caterpillar mixer uses the stretching and folding method by dividing and rejoining. The micromixer has an advantage over the active micromixers and caterpillar mixers in terms of construction. The structures are easily replicated in polymer by injection molding or heat embossing. For folding, the flows are rotated 90 degrees between splitting and rejoining (Tofteberg et al., 2010).A chaotic micromixer with two-layer serpentine crossing channels was proposed to enhance the mixing performance at low Reynolds numbers based on 3D Navier-Stokes equations with a species concentration model of convection-diffusion (Hossain et al., 2017). A micromixer uses only buffer solution and magnetic force to produce a chaotic flow without any barrier structure introduced by (Lee et al., 2009) and provides a reversible rotation that can be utilized to play a part as an active mixer without the usage of any other equipment.

Passive micromixers with microfluidic recirculation in the circular and square mixing chambers were investigated at Reynolds numbers ranging from 0.1 to 75 for two different micromixer designs with eight mixing chambers (circular and square) (Gidde et al., 2018). In the second phase, the mixing performance of two micromixers was evaluated for Reynolds numbers of 0.1 and 75.2 based on the mixing chamber shape.

A numerical study of mixing in different microchannels, zig-zag, square-wave, and curved channels has been conducted by (Hossain et al., 2009). There have been three-dimensional Navier-stokes investigations of mixing and the flow field for a wide range of Reynolds numbers (0.267 to 267). Even at low Reynolds numbers (5 to 15), depending on the kind of microchannels, transverse flow is negligible in all three microchannels. As a result of the longer residence time that results from lower velocity, mixing happens only due to fluid molecule diffusion. So, the mixing gets better as the Reynolds number drops in this area. Passive microfluidic mixer called the ‘‘H-micromixer’’

based on the splitting and recombination (SAR) process describes an experimental investigation of the mixing process in three different geometries: T-micromixer, O-micromixer and H-micromixer (Nimafar et al., 2012). The laminar flow regime (0.08<Re<4.16) was considered during tests, and image-based techniques were used to investigate mixing efficiency. Experimental data shows that H-micromixer is more efficient than the other tested microdevices at all tested flow rates. Two micromixers SESM (Stacking-E-shape micromixer) and FESM (Folding-E-shape micromixer), were investigated using COMSOL Multiphysics 4.4. using the finite element to couple solver to solve the steady-incompressible Navier–Stokes and Convection–Diffusion equations. (Chen & Shen, 2017). Two different types of micromixer cross-sections, circular and rectangular was used in the 3D simulation technique, including the channel's inlet angle, input velocity of fluids, and diffusion coefficient (Farahinia & Zhang, 2020).

In the last few years, a number of different passive mixers have been developed. However, not many investigations have been reported comparing the flow and mixing methods of different geometries. In this study, a numerical investigation is carried out for a novel micromixer based on a Z shape and Ohm shape geometric profile. First, the simulation was experimented with in ANSYS Fluent. Next, the characteristics of the micromixer's outlet velocity and pressure drop with mesh size were investigated numerically and experimentally at a Reynolds number ranging from 50 to 200. Then the performance of the Z & Ohm shape micromixer was compared with the zig-zag shape micromixer in the same conditions.

3. Methodology

This study presents three basic micromixers that were built in order to compare their mixing efficiency with the new microdevice that was presented in this paper. Figure 2 depicts the zig-zag micromixers that have been developed and manufactured. There was no variation in geometric characterization across all prototypes. Two different types of fluid enter the microchannel at two different openings. In terms of design, the Z& Ohm shape micromixer is the most basic microfluidic device, depicted in figure 1 & 3. Both Z and Ohm shape micromixers consist of two inlets connected by a straight channel.

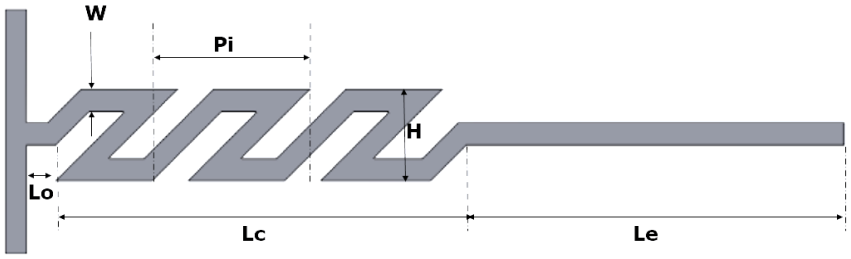

Figure 1: Z shape micromixer

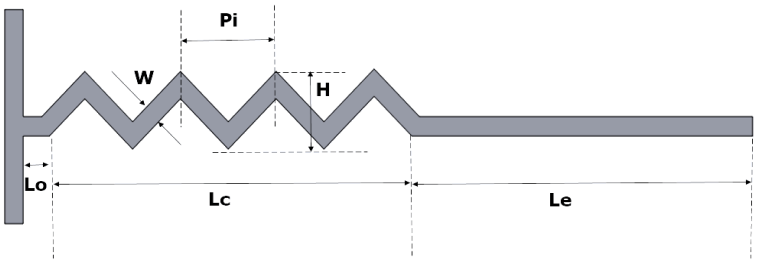

Figure 2: Zig-zag shape micromixer

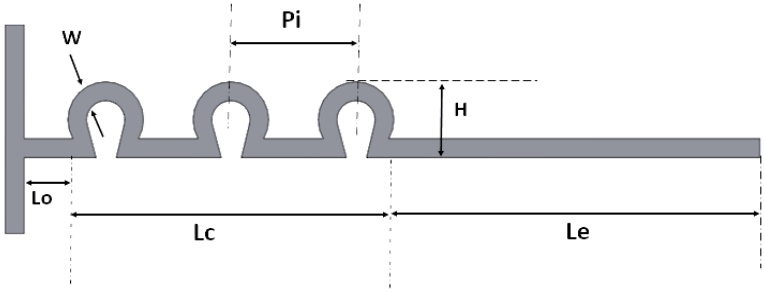

Figure 3: Ohm shape micromixer

To keep things simple for all three geometries, we maintain the same values for the channel height (H), axial length (Lc), width (W), direction length (B), and the number of repeating units (NRUs). The following are the measurements in inches: H is equal to 0.4 mm, Lc is equal to 2.0 mm, W is equal to 0.1 mm, B is equal to 0.1 mm, Pi is equal to 0.56 mm (0.66 mm for Ohm shape), Lo is equal to 0.1 mm, and Le is equal to 1.8 mm. This means that the channel's aspect ratio, W/B, is equal to 1.
There are a total of four repeated units in this composition. The corner angle in the zigzag channel is 90 degrees. 0.1 mm 0.1 mm cross-sectional dimension is shared by the inlet and main channels. Figures 1, 2 and 3 show how a T-joint joins the two inlets, Inlet 1 and Inlet 2 in the main microchannel. As the two mixing fluids, water and ethanol, are employed having characteristics at 20 degrees Celsius. Both water and ethanol have a diffusivity of 1.2 109 m^2/s.

3.1 Simulation

To analyze the flow and mixing in the micromixers, ANSYS Fluent has been used. By using the finite-element method, the ANSYS fluent solves the Navier–Stokes equations. The solver solves the steady continuity and momentum (Navier–Stokes) equations. To get accurate mixing simulations, meshing must be examined and modified and is the main important part of the grid independency test. To analyze the actual mixing phenomena in the microchannels, Navier–Stokes equations in combination with an advection-diffusion model are applied. Through the grid independency test, we will know if the model is being converged or not. We go to mesh sizing & we turn off the “Use advance size function”. It will turn off auto meshing which will help us to get the accurate mesh size.

Next, we go to the mesh method & select the whole body as the geometry & select tetrahedral method. By selecting this method, all the cells will be tetrahedral shape. Then we generate the mesh. We set the behavior of the mesh to hard. Hard behavior helps to get a finer mesh. Element size determines the number of nodes & elements. We can change the number of elements by changing the element size. In the Z (fig 3, a), Zig-zag (fig 3, b) and Ohm (fig 3, c) shape we took several element sizes for different element & node numbers.

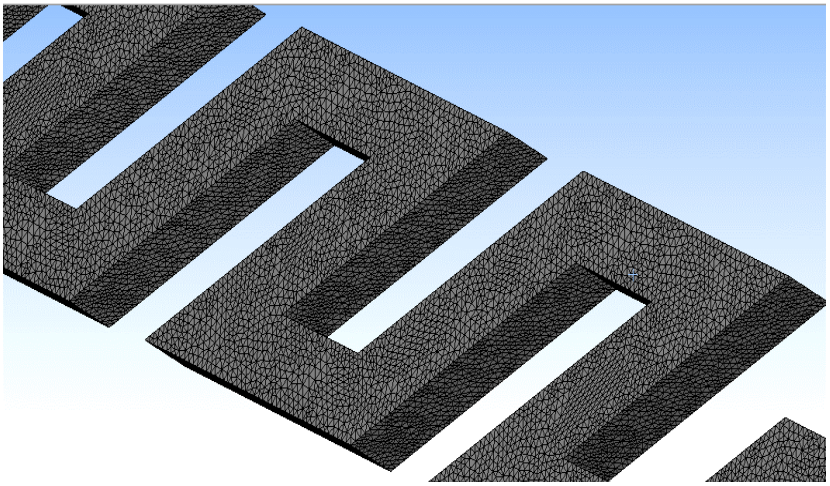

(a)

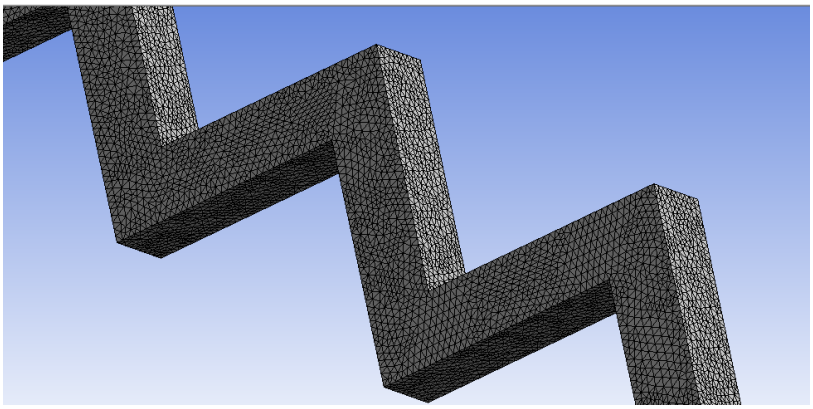

(b)

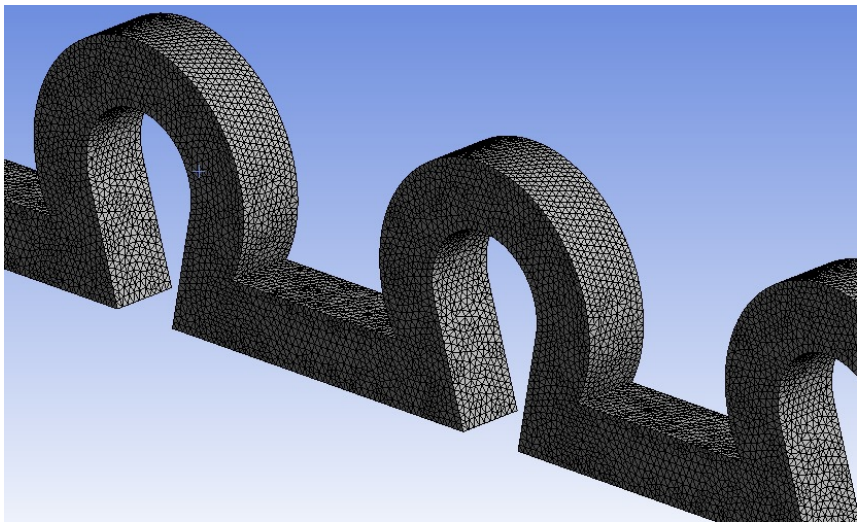

(c)

Figure 3: Tetrahedral grid system: (a) Z shape; (b) Zig-zag shape; (c) Ohm shape

We started with an element size of 0.00001 m for the Z shape to see how it would work shown in table 1. This mesh was generated using 681186 elements and 131593 nodes for the Z shape and elements and nodes for the Ohm shape (580434 elements and 111811 nodes). We obtained 6034 elements and 1817 nodes for the Z shape and 5266 elements and 1606 nodes for the Ohm form for an element size of 0.00005 *m*. We got 3307 elements and 1229 nodes for the Z shape and 1068 elements and 2816 nodes for the Ohm form for an element size of 0.00006*m*. For the Zig Zag shape, the element number & nodes are 516381 & 99513 respectively, for the element size of 0.00001*m*. Number of elements & nodes are 4727 & 1403 respectively for 0.00005*m* element size. Finally, elements & nodes are 2465 & 936 for 0.00006*m* element size.

Table 1: Number of elements and Nodes

Shapes	Mesh Size (*m*)	Elements	Nodes
Z	0.00001	681186	131593
	0.00005	6034	1817
	0.00006	3307	1229
Ohm	0.00001	580434	111811
	0.00005	5266	1606
	0.00006	1068	2816
Zig zag	0.00001	516381	99513
	0.00005	4727	1403
	0.00006	2465	936

After the meshing, we got to select the inlets, outlet & fluid domain. By clicking the inlet face surface, we select inlet 1 & 2 respectively and same for the outlet. For the fluid domain, we have to select the whole body & then rename it the fluid domain.

For setup, we must choose double precision and serial processing as our processing options. After that, we begin the installation process. To begin the setup process, we must first configure the models. Multiphase must be turned off; the energy equation must be activated, and viscous must be laminar. The remainder of the models must be taken out of the picture. After that, we will have to decide on the materials. Because our passive micromixer has two inlets, we choose water and ethanol as the two liquids for the two inlets. Water is used for inlet one, and ethanol is used for inlet 2 of the system. We used water and ethanol at a temperature of 20° C. From the table 2, we got the values such as water has a density of 998 kg/m^3 and ethanol has a density of 790 kg/m^3 and dynamic viscosity is 0.0010016 Nsm^{-2} and 1.144×10^3 Nsm^{-2} respectively

Table 2: Properties of fluids at 20^0C

Fluid	Density (kgm^{-3})	Viscosity (Nsm^{-2})	Diffusivity (m^2s^{-1})
Water	998	0.9×10^{-3}	1.2×10^{-9}
Ethanol	790	1.2×10^{-3}	1.2×10^{-9}

In order to create the cell zone condition, we must first choose the material for the fluid domain. It is now time to discuss the boundary condition, which is the most critical aspect of a flow simulation. This set of boundary conditions has an impact on all of the results. The boundary condition solves all governing equations using finite element analysis Finite Element Analysis (FEA). We choose the velocity of the inlet one boundary condition as the boundary condition for the inlet one boundary condition. We need to know the velocity of the water because it is passing through inlet 1. To determine the velocity, we choose a given Reynolds number. We know that Reynold's number depends on the density, velocity, diameter of the microchannel, and the fluid's dynamic viscosity. Then used three distinct sorts of Reynolds' numbers for three different input and output velocities, and we averaged them out. First, we picked 0.5, then 50, and finally 200 as a starting point.

$$R_e = \frac{\rho V D}{\mu}$$

Here,
ρ= Density of the fluid
V= Velocity of the fluid at inlet
D= Diameter of the microchannel
μ= Dynamic viscosity of the fluid

By putting Re=0.5 we get the velocity $0.00501 ms^{-1}$ for water at inlet 1. For ethanol at inlet 2, we get the inlet velocity of $0.00724 ms^{-1}$. We put this velocity in the inlet boundary condition. Similarly, when we take Re=50 the velocity becomes 0.5001 & $0.724 ms^{-1}$ respectively. When $R_e = 200$ the velocity is 2 & $2.89 ms^{-1}$. In outlet boundary conditions, the gauge pressure is 0 Pa at the end of the microchannel. As the fluid passes through the channel, pressure starts to drop & become zero at the end of the tip. For the wall fluid domain boundary condition, we keep the wall motion stationary and no-slip wall condition is being applied keeping the dynamic meshing off.

3.2 Results and Discussions

Following the completion of the simulation, it is necessary to verify that the response is not dependent on the number of grids used to establish the optimal number of grids to employ. We examined three distinct structured grid systems (fig 4, a), whose number of grids varied from 2.01105 to 1.65106 for each microchannel, with the number of grids ranging from 2.01105 to 1.65106. Finally, according to the findings of the grid-dependency test, the value 1.12 106 was chosen.

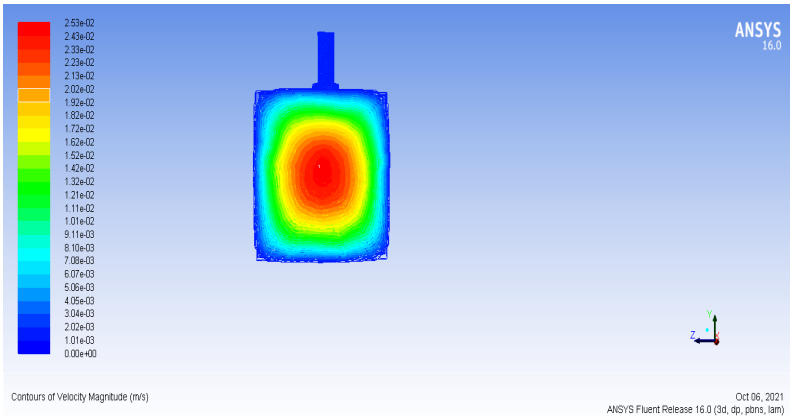

(a)

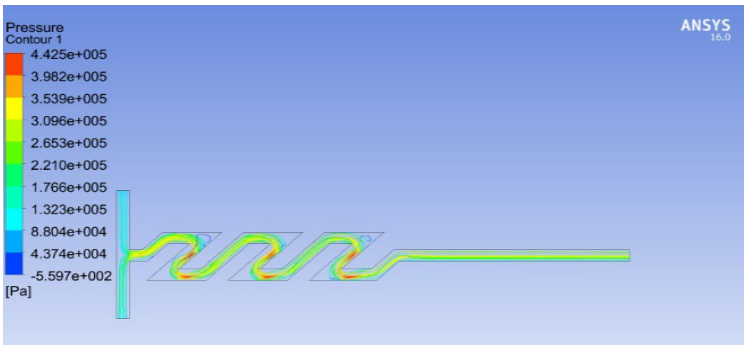

(b)

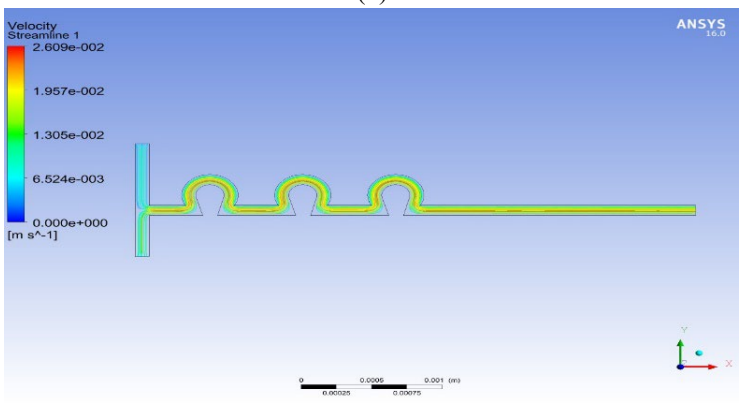

(c)

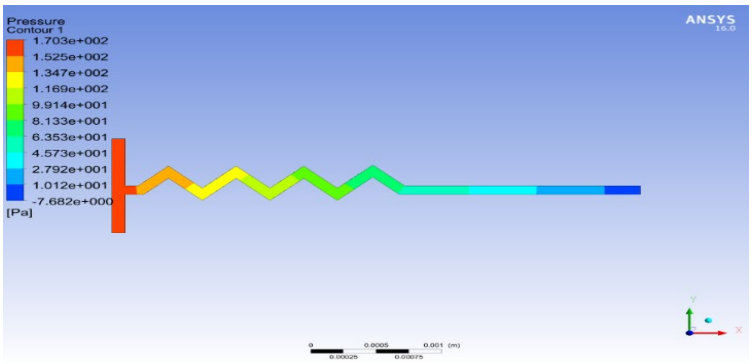

(d)

Figure 4: Simulation results: (a) Velocity gradient for Z shape; (b) Pressure counter1 for Z shape; (c) Velocity streamlines for Ohm shape; (d) Pressure counter1 for Zig zag shape

The simulation for different grid numbers with different Reynolds number to find out the outlet velocity gradient (fig 4, a) and pressure counter (fig 4, b) for Z shape at inlets and boundary wall. In (fig 4, c), we ran the simulation for velocity streamlines of Ohm shape and the pressure counter for Zig zag shape is depicted in the (Fig 4, d). The results are plotted as outlet velocity vs Reynolds number for Z shape (fig 5, a), Ohm shape (fig 5, b) and Zig-zag shape (fig 5, c) respectively.

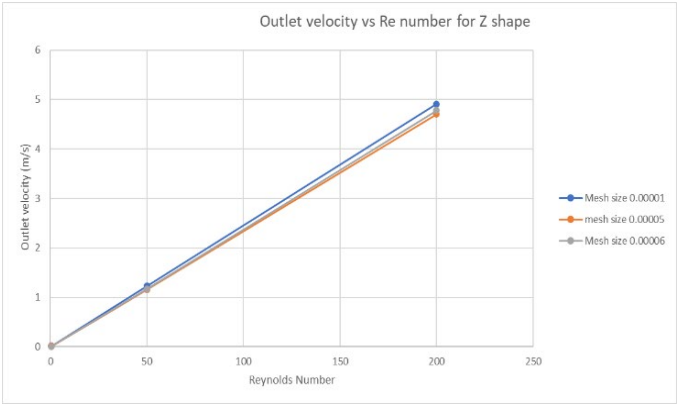

(a)

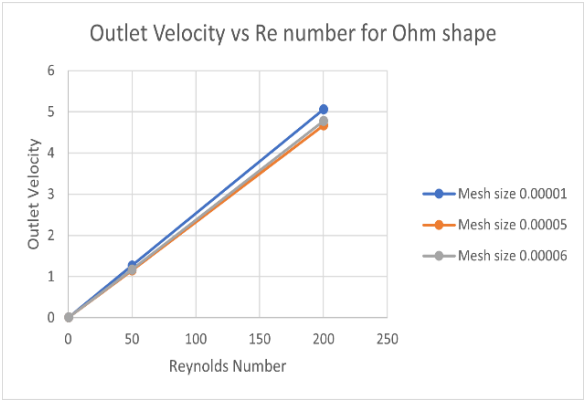

(b)

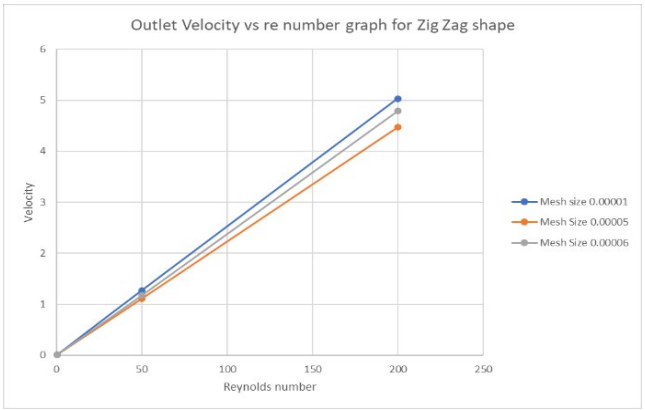

(c)

Figure 5: Outlet velocity vs Re number: (a) for Z shape; (b) for Zig-zag shape; (c) for Ohm shape

The outlet velocity increases as the Reynolds number grows for each grid number for both the Z (fig 5, a), Ohm shape (fig 5, b) and zig-zag (fig 5, c) shapes, and that the velocity differential between the outlet and inlets is substantially greater for the optimally selected grid numbers.

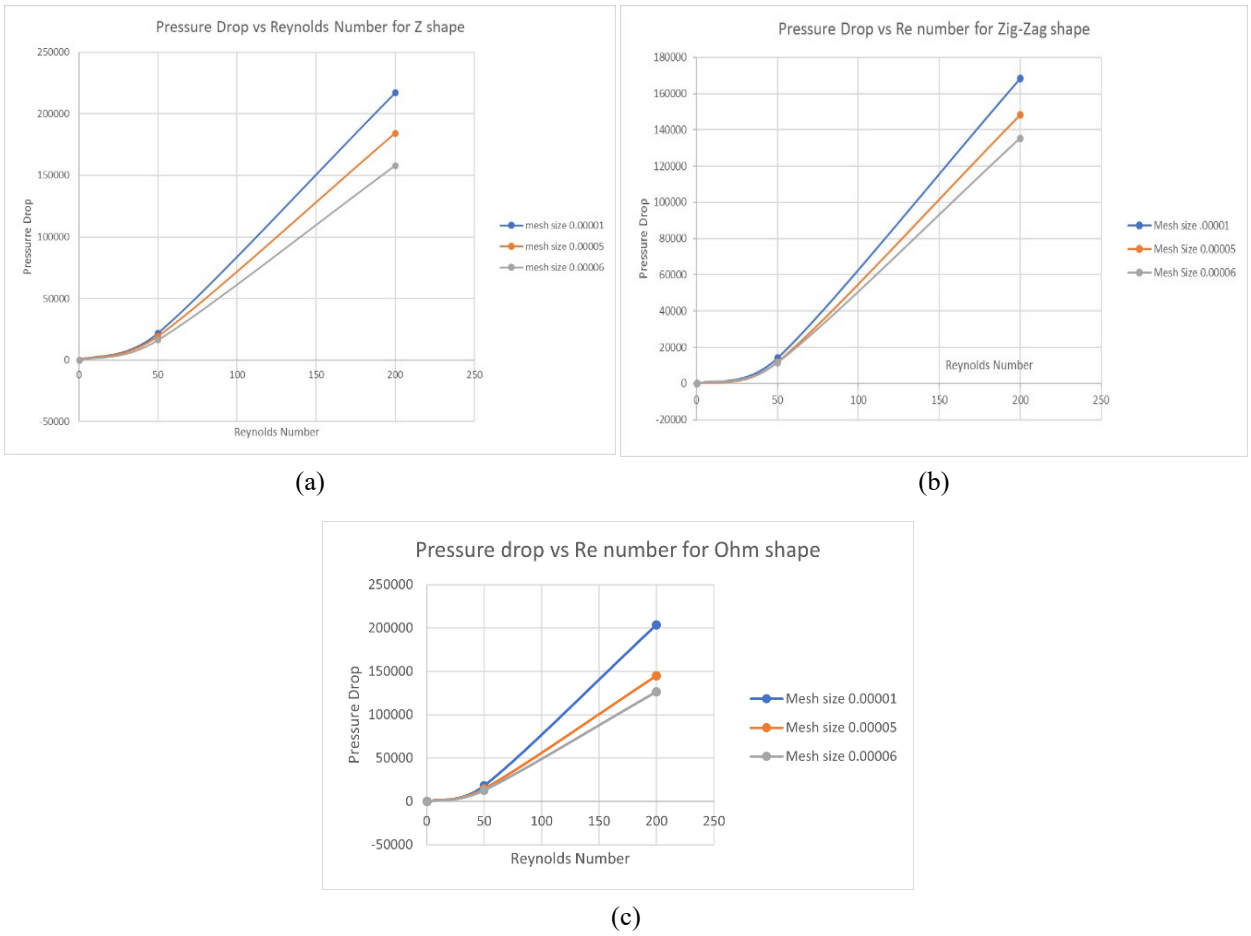

(a) (b)

(c)

Figure 6: Pressure drop vs Re number: (a) Z shape; (b) Zig zag shape; (c) Ohm shape

Pressure drop vs Reynolds numbers for various shapes are presented on the screen for Z shape (fig 6, a), Zig-zag shape (fig 6, b) and Ohm shape (fig 6, c). The pressure drop is greatest for mesh sizes of 0.00001 in different Reynolds numbers, and that it is lowest for mesh sizes of 0.00006, indicating that the pressure drop is greatest for the optimal grid numbers (0.00001 in different Reynolds values).

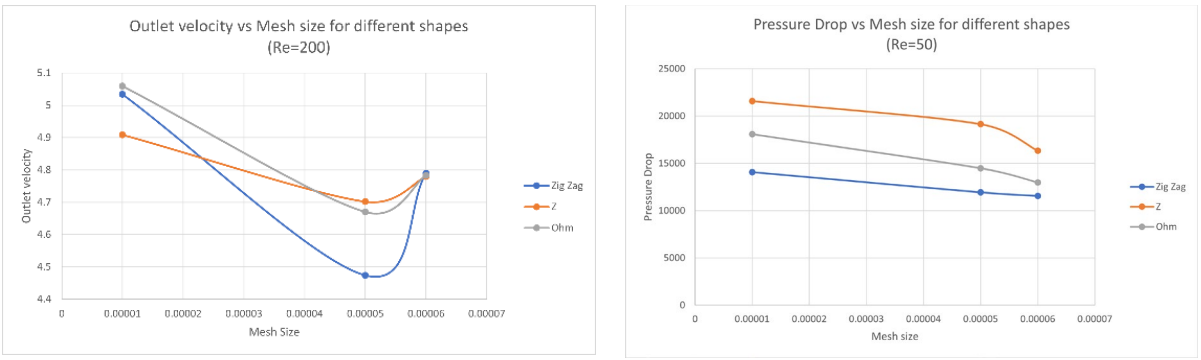

(a) (b)

Figure 7: (a) Outlet velocity vs mesh size; (b) Pressure drop vs mesh size

Outlet velocity vs mesh size is plotted for all three shapes with a constant Reynolds number of 200 (fig 7, a). The outflow velocity of the zig-zag form decreases dramatically as compared to the Z and Ohm shape as the mesh size increases until it reaches the ideal mesh size of 0.00006, which is the smallest possible. According to the graph (fig 7, b), the pressure drop for the zig-zag form is consistently lower than the pressure drop for the Ohm shape while it is maximum for Z shape, indicating that the pressure profile is comparatively better in the Ohm and Zig-zag shape.

At an Ideal mesh size of 6×10^{-5} *m* the is mixing performance of Z shape and Ohm shape micromixer was compared to a zig-zag shape micromixer placed equally along the micromixer's length. The geometric design variable has an effect on Reynolds numbers ranging from 50 to 200 in the mixing and flow fields where the mixing performance is better with higher Reynolds numbers. The Zig-zag micromixer produced less pressure drop than the Z shape and Ohm shape micromixer while the Z and Ohm shape micromixer give much more stable velocity profile.

4. Conclusion

The mixing performance of Z and Ohm shape micromixer compared to zig-zag shape micromixer placed equally along the micromixer's length was investigated using computational methods. The mixing and flow fields were examined to determine how Reynolds numbers ranging from 50 to 200 are affected by the geometric design variable. For more significant Reynolds numbers, the micromixer had better mixing results. At Re=200, the mixing performance improved to its greatest extent. Compared to the Z and Ohm shape micromixer, the pressure drop produced by the zig-zag shape micromixer was lower. As a result, the pumping power required by the micromixer is lower. Thus, the proposed shape provides more stable velocity for mixing and in future work the mixing index will be calculated for all the shapes and will be compared the results to get the efficient shape of micromixer.

References

Anwar, K., Han, T., Yu, S., & Kim, S. M. (2010). An integrated micro-nanofluidic system for sample preparation and preconcentration of proteins. *14th International Conference on Miniaturized Systems for Chemistry and Life Sciences 2010, MicroTAS 2010*, *1*(October), 443–445.

Chen, X., & Shen, J. (2017). Numerical analysis of mixing behaviors of two types of E-shape micromixers. *International Journal of Heat and Mass Transfer*, *106*, 593–600. https://doi.org/10.1016/j.ijheatmasstransfer.2016.09.034

Farahinia, A., & Zhang, W. J. (2020). Numerical analysis of a microfluidic mixer and the effects of different cross-sections and various input angles on its mixing performance. *Journal of the Brazilian Society of Mechanical Sciences and Engineering*, *42*(4). https://doi.org/10.1007/s40430-020-02275-9

Gidde, R. R., Pawar, P. M., Ronge, B. P., Misal, N. D., Kapurkar, R. B., & Parkhe, A. K. (2018). Evaluation of the mixing performance in a planar passive micromixer with circular and square mixing chambers. *Microsystem Technologies*, *24*(6), 2599–2610. https://doi.org/10.1007/s00542-017-3686-0

Hossain, S., Ansari, M. A., & Kim, K. Y. (2009). Evaluation of the mixing performance of three passive micromixers. *Chemical Engineering Journal*, *150*(2–3), 492–501. https://doi.org/10.1016/j.cej.2009.02.033

Hossain, S., Lee, I., Kim, S. M., & Kim, K. Y. (2017). A micromixer with two-layer serpentine crossing channels

having excellent mixing performance at low Reynolds numbers. *Chemical Engineering Journal*, *327*, 268–277. https://doi.org/10.1016/j.cej.2017.06.106

Jeon, M. K., Kim, J. H., Noh, J., Kim, S. H., Park, H. G., & Woo, S. I. (2005). Design and characterization of a passive recycle micromixer. *Journal of Micromechanics and Microengineering*, *15*(2), 346–350. https://doi.org/10.1088/0960-1317/15/2/014

Kashid, M. N., & Agar, D. W. (2007). Hydrodynamics of liquid-liquid slug flow capillary microreactor: Flow regimes, slug size and pressure drop. *Chemical Engineering Journal*, *131*(1–3), 1–13. https://doi.org/10.1016/j.cej.2006.11.020

Kim, K., Ansari, M. A., & Afzal, A. (2018). Passive Micromixers. In *Passive Micromixers*. https://doi.org/10.3390/books978-3-03897-008-8

Le The, H., Le Thanh, H., Dong, T., Ta, B. Q., Tran-Minh, N., & Karlsen, F. (2015). An effective passive micromixer with shifted trapezoidal blades using wide Reynolds number range. *Chemical Engineering Research and Design*, *93*, 1–11. https://doi.org/10.1016/j.cherd.2014.12.003

Lee, S. H., Kang, H. J., & Choi, B. (2009). A study on the novel micromixer with chaotic flows. *Microsystem Technologies*, *15*(2), 269–277. https://doi.org/10.1007/s00542-008-0664-6

Manoj Dundi, T., Chandrasekhar, S., Rampalli, S., Raju, V. R. K., & Chandramohan, V. P. (2020). Numerical analysis of liquid mixing in a T -micromixer with taylor dispersion obstructions. *International Journal of Mathematical, Engineering and Management Sciences*, *5*(1), 147–160. https://doi.org/10.33889/IJMEMS.2020.5.1.013

Nimafar, M., Viktorov, V., & Martinelli, M. (2012). Experimental comparative mixing performance of passive micromixers with H-shaped sub-channels. *Chemical Engineering Science*, *76*, 37–44. https://doi.org/10.1016/j.ces.2012.03.036

Tofteberg, T., Skolimowski, M., Andreassen, E., & Geschke, O. (2010). A novel passive micromixer: Lamination in a planar channel system. *Microfluidics and Nanofluidics*, *8*(2), 209–215. https://doi.org/10.1007/s10404-009-0456-z

Viktorov, V., & Nimafar, M. (2013). A novel generation of 3D SAR-based passive micromixer: Efficient mixing and low pressure drop at a low Reynolds number. *Journal of Micromechanics and Microengineering*, *23*(5). https://doi.org/10.1088/0960-1317/23/5/055023

Biographies

Moddassir Khan Nayeem

He is a lecturer at the department of Industrial and Production Engineering (IPE) of Military Institute of Science and Technology. He completed his master's in Industrial Engineering from Pusan National University, South Korea and bachelor's degree in IPE from Ahsanullah University of Science and Technology. His research interest largely focusing on Operations research. He works as an Editorial assistant at the International Journal of Industrial Engineering: Theory, Applications and Practice. He also serves as a reviewer for the several reputed international journals.

Zubairul Alam is a student of Military Institute of Science & Technology. He is studying Industrial and Production Engineering and is currently enrolled in 4th year. He earned both of her Secondary & Higher Secondary School Certificates from Dhaka Board. His research interests include manufacturing, simulation, optimization, 3D printing, additive manufacturing, supply chain management, and lean. He is serving as the director of webmaster of the IEOM student chapter of Military Institute of Science & Technology.

S M Faisal Ahmmed is a student of the Department of Industrial & Production Engineering at Military Institute of Science & Technology, Dhaka, Bangladesh and is currently enrolled in 4th year. He holds the Professional certification on High Potential Graduate Preliminary by CKH network. He's interested in the fields of Additive Manufacturing, 3d Printing, Manufacturing, Lean, Logistic, Transport and Supply Chain Management. He is very much interested to be a part of IEOM.

Tanveer Rahman is a student of Military Institute of Science & Technology. He is studying Industrial and Production Engineering and is currently enrolled in 4th year. He earned his Higher Secondary School Certificates from Govt. Hazi Mohammod Mohsin College, Chiitagong board. His research interests include manufacturing, modeling &

simulations, optimization, 3D printing, additive manufacturing, supply chain management, Operations Management, and lean Manufacturing. He is very much interested to be a part of IEOM.